Sensors & Diagnostics

PAPER

View Article Online
View Journal | View Issue

Cite this: *Sens. Diagn.*, 2024, **3**, 1044

Effects of storage conditions on the performance of an electrochemical aptamer-based sensor†

Julia Chung, [a] Adriana Billante,[b] Charlotte Flatebo, [c] Kaylyn K. Leung, [bd] Julian Gerson,[de] Nicole Emmons,[de] Tod E. Kippin,[ae] Lior Sepunaru [b] and Kevin W. Plaxco *[abcd]

Received 28th February 2024,
Accepted 11th April 2024

DOI: 10.1039/d4sd00066h

rsc.li/sensors

The electrochemical aptamer-based (EAB) sensor platform is the only molecular monitoring approach yet reported that is (1) real time and effectively continuous, (2) selective enough to deploy *in situ* in the living body, and (3) independent of the chemical or enzymatic reactivity of its target, rendering it adaptable to a wide range of analytes. These attributes suggest the EAB platform will prove to be an important tool in both biomedical research and clinical practice. To advance this possibility, here we have explored the stability of EAB sensors upon storage, using retention of the target recognizing aptamer, the sensor's signal gain, and the affinity of the aptamer as our performance metrics. Doing so we find that low-temperature (−20 °C) storage is sufficient to preserve sensor functionality for at least six months without the need for exogenous preservatives.

Introduction

The ability to measure molecules in the body in real time and at high frequency would advance both biomedical research and clinical practice. By providing such information on blood sugar, for example, the continuous glucose sensor has transformed the management of diabetes.[1–4] Unfortunately, however, the operation of the glucose sensor is reliant on an enzyme that converts its target into an easily detectable product, rendering the approach difficult to generalize to analytes for which an appropriate enzyme is not available. In response, recent years have seen the development of electrochemical aptamer-based (EAB) sensors, an *in vivo* molecular measurement technology that does not rely on the chemical transformation of its targets, thus rendering it easily adaptable to new analytes. To achieve this, EAB sensors consist of a redox-reporter-modified aptamer (target-binding oligonucleotide) chemisorbed to a gold electrode through alkanethiol self-assembly (Fig. 1A).[5–8] In the absence of target, the aptamer exists in dynamic equilibrium and takes a predominantly unfolded state where the redox reporter is far from the gold surface, leading to relatively slow electron transfer.[9] Upon target addition, the aptamer undergoes binding-induced folding, moving the redox reporter closer to the gold surface and accelerating electron transfer. With electrochemical interrogation, the sensor exhibits a target-dependent current change. Using such sensors, we and others have achieved sub-second resolution in the measurement of drugs, metabolites, and other small molecules over the course of hours *in situ* in the blood, brains, and peripheral tissues of live animals.[10–16] Despite this advantage, shelf-life remains a relatively underexplored and potentially serious obstacle to the wide-spread use of EAB sensors. Specifically, we have historically fabricated EAB sensors and used them within 24 h rather than manufacturing them in bulk for future use. Here, however, we explore EAB sensor storage by monitoring the performance of such sensors after prolonged periods under various conditions.

While several elements of an EAB sensor might be labile to storage (*e.g.*, their redox reporter,[17] the nanodendrite structure of their gold electrodes,[18,19] and the DNA aptamer[20]), perhaps the most labile of their components is the self-assembled alkanethiol monolayer (SAM) used to attach the target-recognizing aptamer to the interrogating electrode.[8] Specifically, it is known that such SAMs can desorb,[21,22] degrading sensor performance and leading to efforts to address this problem. Given this, in an early effort to preserve EAB sensors we found that increasing the length

[a] *Interdepartmental Program in Biomolecular Science and Engineering, University of California Santa Barbara, Santa Barbara, California 93106, USA. E-mail: kwp@ucsb.edu*
[b] *Department of Chemistry and Biochemistry, University of California Santa Barbara, Santa Barbara, California 93106, USA*
[c] *Institute for Collaborative Biotechnologies, University of California Santa Barbara, Santa Barbara, California 93106, USA*
[d] *Center for Bioengineering, University of California Santa Barbara, Santa Barbara, California 93106, USA*
[e] *Department of Psychological and Brain Sciences, University of California Santa Barbara, Santa Barbara, California 93106, USA*

† Electronic supplementary information (ESI) available. See DOI: https://doi.org/10.1039/d4sd00066h

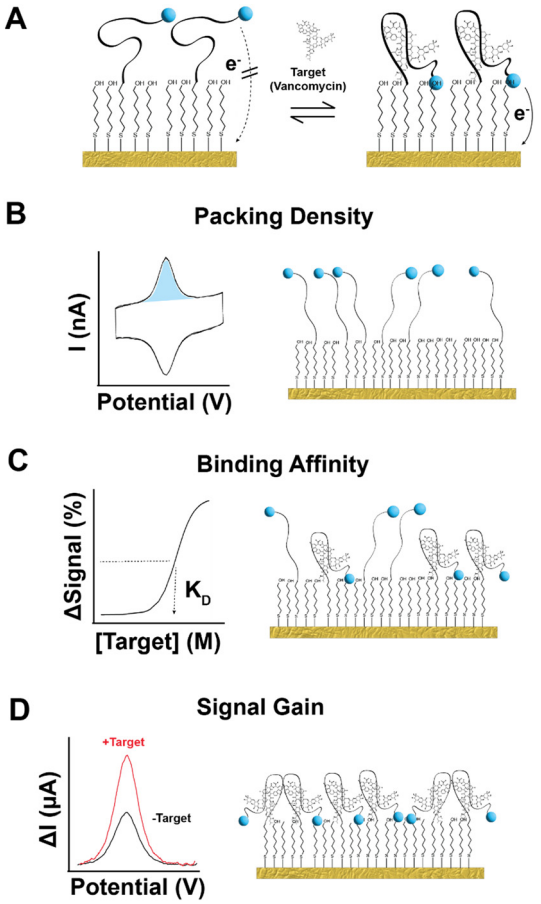

Fig. 1 EAB sensors, which support real-time molecular measurements *in situ* in the body, are comprised of a gold surface upon which we attach a thiol-and-redox-reporter-modified aptamer. Here, as our test bed, we have used a sensor against vancomycin, which is employs a 45-base aptamer specific for this antibiotic.[31] The 5′-end of this aptamer is modified to contain a 6-carbon thiol linker, which attaches to the surface of the gold interrogating electrode through self-assembly.[32] We then introduce 6-mercapto-1-hexanol to complete a densely packed monolayer. (A) In the absence of target, the unfolded aptamer results in slower electron transfer rate from the reporter (here methylene blue). Upon the addition of target, the aptamer folds, accelerating the rate of electron transfer. Square-wave voltametric interrogation of this system yields a peak current, the amplitude of which changes in a target-concentration dependent manner. Measurable parameters of EAB performance impacted by storage include (B) how many aptamers are present on the sensor surface, (C) the target concentration at which the sensor's signal change hits its midpoint (K_D), and (D) the sensor's signal gain (relative change in signal from zero to saturating concentration of target). Here we have determined the extent to which each of these parameters change over time under a range of relatively convenient storage conditions.

of the alkanethiol from 6- to 11-carbon extends the period over which the sensor retains good signal-to-noise ratios upon room-temperature storage.[23] This improved stability, however, comes at the cost of reduced signaling currents and eliminating the "signal-off" low-square-wave-frequency response required to correct the drift inevitably seen *in vivo*.[10,24,25] Concurrently, we reported in the same work that the addition of 5% w/v bovine serum albumin (BSA) and trehalose[26] improves the stability of both 6- and 11-carbon alkanethiol EAB sensors against storage for up to 30 days under dry, room temperature conditions.[23] In a second example, Phares and coworkers enhanced monolayer stability *via* a flexible trihexylthiol,[27,28] finding that sensors fabricated using this linker exhibit a loss of only 20% in peak current after 50 days of storage, *versus* the 60% loss seen for sensors fabricated with alkanethiols or rigid trithiols. Finally, Heikenfeld and co-workers have shown that the addition of bovine serum albumin and trehalose can preserve alkanethiol-based EAB performance for at least 7 days under dry storage conditions.[29,30] Expanding on this prior work, here we explore storage conditions obviating the need for such exogenous preservatives, finding that storage in phosphate buffered saline (PBS) at −20 °C extends the shelf-life of EAB sensors to at least 6 months.

Results and discussion

We investigated the stability of EAB sensors by employing an established vancomycin-detecting device[31] comprised of a 45-base DNA aptamer covalently modified with a methylene blue redox reporter and attached to a gold electrode *via* an alkanethiol-on-gold self-assembled monolayer (Fig. 1A). We assessed the post-storage performance of this sensor using three metrics. The first was retention of the target-binding aptamer on the sensor surface. To determine this, we monitored the change in the number of redox-reporter-modified aptamers (as measured by total charge transfer *via* cyclic voltammetry) from immediately after sensor fabrication to each measurement timepoint during storage (Fig. 1B). For our second performance metric, we assess the reproducibility of the sensor's affinity for its target, as defined by the midpoint of its binding curve (Fig. 1C). Our final performance metric is the reproducibility of the sensor's signal gain; that is, the relative change in signal seen upon transitioning from no target to a saturating concentration of target (Fig. 1D). To determine signal gain and binding midpoint, we perform titrations, monitoring the sensor's response using kinetic differential measurements (KDM)[10,25] a square wave voltammetry approach employed to correct the drift seen in *in vivo* measurements. In this analysis, we choose a pair of square-wave frequencies that exhibit the same current decay over time required to perform the titration, thus restoring the baseline to a slope of zero.

We first assessed sensor performance at room temperature under dry storage and storage immersed in PBS, finding that such conditions cause significant aptamer loss in as little as 7 days. To see this, we fabricated and stored a set of 32 electrodes under 8 permutations of the following conditions: dry (dried from PBS) or wet (stored under PBS), with or without the addition of 35 mM 6-mercapto-1-hexanol (in the PBS from which the sensor was dried or in which it was stored), and with or without argon sparging to reduce the presence of molecular oxygen. Prior to storage, the average initial packing density (number of redox reporters per unit

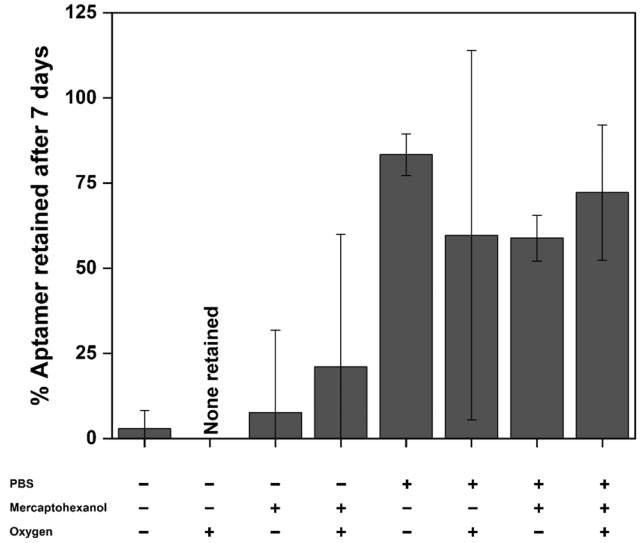

Fig. 2 Room temperature storage leads to significant loss in aptamer (as monitored by the density of redox reporters), especially for dry storage conditions. Here, we assess this retention after 7 days of storage in the presence and absence of PBS buffer (*i.e.*, wet or dry), the presence and absence of 35 mM 6-mercapto-1-hexanol (in the PBS used for wet storage or from which the sensor was dried), and the presence or absence of oxygen, which is removed *via* argon sparging. In the presence of buffer, we found that neither sparging nor the presence of 6-mercapto-1-hexanol significantly improved aptamer retention. Error bars represent 95% confidence intervals.

area) of our vancomycin-detecting sensors is 9.5 (±0.8) × 10^9 aptamers per mm^2, their average signal gain is 95 (±4)% and their average binding midpoint is 17 (±1) μM (Fig. S1†); we provide 95% confidence intervals for each parameter to identify statistically significant differences before and after storage. After 7 days storage at room temperature under buffer, between 50–80% of the initial packing density remains, with neither the addition of 6-mercapto-1-hexanol, which we introduced in the expectation that it might reverse monolayer desorption,[33–35] nor the removal of oxygen, which we expected might reduce oxidative desorption of the SAM,[36–39] improving aptamer retention (Fig. 2). All four of our dry storage conditions faired even more poorly, resulting in loss of more than 75% of the initial aptamer load. Of note, the aptamer loss observed under dry storage conditions arises due to storage and not due to the drying process itself: we do not observe any significant change in packing density when we immediately (<15 min) return dried sensors to buffer for testing (Fig. S2†).

In contrast to room temperature sensor storage, EAB sensor performance remains excellent even after six months of storage at −20 °C. To perform this study, we initially screened sensors stored under PBS buffer for 7 days at room temperature (20 °C), in the refrigerator (4 °C), or in the freezer (−20 °C), finding the best retention of performance under the last of these three conditions (Fig. S3†). To better explore the performance of individual sensors over time when stored under these conditions, we next challenged a single set of eight sensors with electrochemical testing over the course of a month. Here, we interrogated each sensor at multiple timepoints, allowing each to equilibrate to room temperature prior to its interrogation, after which it was returned to storage for later re-testing. As a control for losses that may result from electrochemical interrogation,[22] we subjected a second set of electrodes to the same storage period and number freeze–thaw cycles without electrochemically interrogating them until the final time point. We found little difference in aptamer retention between pre-storage control sensors and post-storage frozen sensors (Fig. 3A). Similarly, we found no statistically significant differences in the signal gains of freshly made sensors, frozen stored sensors interrogated multiple times, and frozen stored sensors interrogated only once (Fig. 3B).

After obtaining promising performance with a single set of EAB sensors stored at −20 °C, we next initiated a long-term study starting with a set of 32 sensors. Prior to storage (day

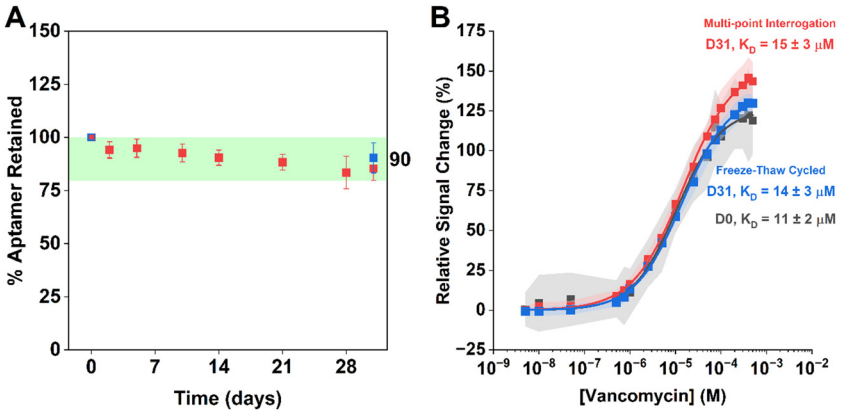

Fig. 3 A set of 8 EAB sensors, each stored frozen at −20 °C and then repeatedly thawed and interrogated over the course of 31 days (red) perform similarly to their fresh counterparts (grey) and to another set of 8 sensors that underwent the same number of freeze–thaw cycles without interrogation until the final day of storage (blue). We observe no statistically significant differences in (A) retention of the target-binding aptamer nor in (B) signal gain and binding midpoints after 31 days of storage under these conditions. Here we employed KDM using square wave frequencies of 10 and 300 Hz.

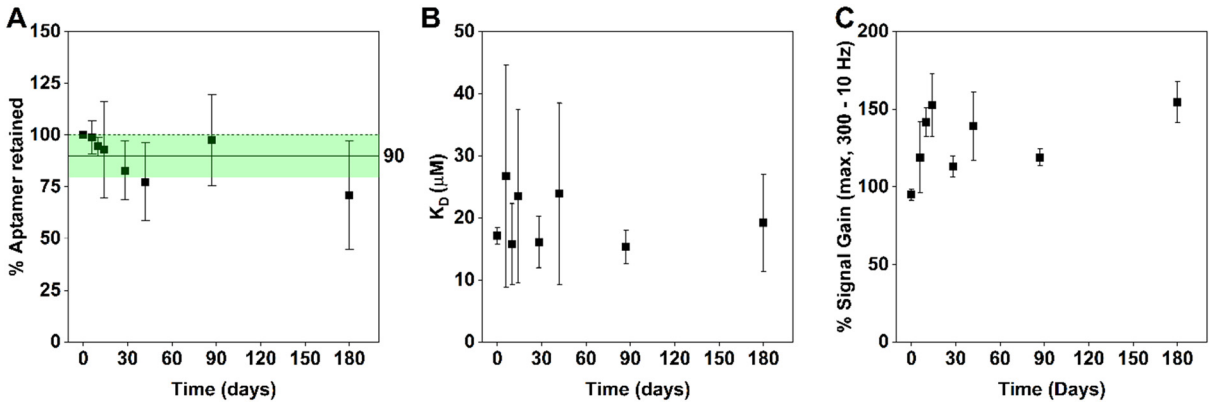

Fig. 4 We see no statistically significant evidence that the performance of vancomycin-detecting EAB sensors changes after storage at −20 °C in PBS without 6-mercapto-1-hexanol. Specifically, (A) aptamer retention and (B) binding midpoints remain constant (to within 95% confidence bounds) over 6 months of storage under these conditions. While (C) signal gain increases slightly upon freeze/thaw, it too remains constant. In contrast to Fig. 3 which follows a single set of 8 sensors over 31 days, Fig. 4 measures four different sensors at each timepoint.

0), we measured the aptamer packing density of all 32 sensors. Then, after storage for a given period, we removed 4 sensors, let them equilibrate to room temperature for 30 min, and characterized their performance. After this testing we retired the four sensors (*i.e.*, did not test them a second time). To determine the percentage of aptamer retained, we normalized the packing density of each sensor following storage to its own packing density as measured on day 0. In doing this, we found that upon storage the aptamer retention (Fig. 4A), binding midpoint (Fig. 4B), and signal gain (Fig. 4C) of these sensors remain effectively unchanged (*i.e.*, within 95% confidence intervals) for at least 6 months. This data suggests that −20 °C storage is sufficient to retain good EAB sensor performance over extended periods.

EAB sensors stored at −20 °C perform similarly to their freshly fabricated counterparts when challenged *in vitro* in undiluted blood held at 37 °C. To see this, we first prepared a set of 3 sensors, determined their "day 0" packing densities, and then stored them at −20 °C for 14 days. After this, we fabricated another set of 3 sensors to act as our fresh sensor control. We then equilibrated all 6 sensors in whole bovine blood for 1 h at 37 °C before spiking the blood with increasing concentrations of the vancomycin target over 15 min intervals. We then returned the sensors to target-free blood. The response of the two sets of sensors to these challenges were within experimental error (Fig. 5).

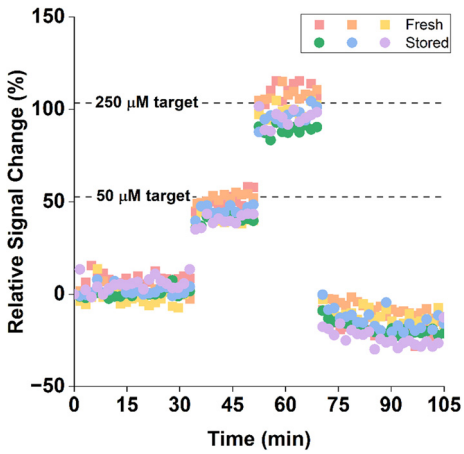

Fig. 5 Stored (green, blue, purple) and fresh (red, orange, yellow) sensors respond similarly when challenged *in vitro* in whole bovine blood held at 37 °C. Due to the difference in temperature and sample matrix, the magnitude of these responses are not comparable to the titration curve presented in Fig. 3; see Fig. S4† for the appropriate calibration curve. Here we employed KDM using square wave frequencies of 10 and 300 Hz.

Conclusion

Wide-spread clinical implementation of EAB sensors requires the ability to transport and store them for extended lengths of time. Here, we explored easily accessible storage conditions, finding that storage at −20 °C for at least 6 months does not significantly decrease aptamer retention or aptamer affinity, nor does it alter the gain of EAB sensors. These findings indicate that the transition of EAB sensors from the site of fabrication to other academic laboratories or to real-world clinical settings can be facilitated by cold storage for protracted periods of time.

Materials & methods

Materials

We fabricate vancomycin-binding sensors using a previously reported,[31,40] vancomycin-binding aptamer of sequence: 5′-SS-$(CH_2)_6$-CGA GGG TAC CGC AAT AGT ACT TAT TGT TCG CCT ATT GTG GGT CGG-methylene blue-3′ (IDT).

All commercially obtained reagents were used as received. We prepared phosphate buffered saline (PBS) at pH 7.4 for use in sensor fabrication by dilution of a stock of 20X PBS (ChemCruz, SC-362299). For subsequent electrochemical tests, we employed phosphate buffered saline at pH 7.4 with the addition of 2 mM $MgCl_2$ (from 1 M stock from Boston BioProducts, BM-670). The bovine blood was commercially

sourced (Hemostat Laboratories) and thus experiments employing it are not subject to institutional review board (IRB) approval.

Sensor fabrication

We prepared gold wire working electrodes as previously described.[8,41] In brief, we soldered a 2.5 cm length of 0.2 mm diameter gold wire to a gold-plated pin connector with 60/40 lead-selenium solder. We encased this electrode using polyolefin shrink-wrap insulation, leaving a 3.1 mm length of bare gold surface. We then trimmed the gold surface to 3 mm. To electrochemically clean this construct, we cycled the potential from −1 V to −1.8 V at a scan rate of 1 V s^{-1} in 0.5 M NaOH for 500 cycles to remove any contaminating organics. These electrodes are then roughed in 0.5 M H_2SO_4 to increase the surface area by stepping the potential between 0 and 2.2 V using a previously described procedure. We found the electroactive electrode area by monitoring the gold oxide reduction peak in 0.05 M H_2SO_4 using cyclic voltammetry.

We then modified the electrode with probe aptamer, as detailed. A stock solution of the aptamer (0.1 mM) was thawed from storage at −20 °C. We incubate this solution in the dark for 1 hour with 6 mM of tris(2-carboxyethyl) phosphine hydrochloride (Sigma Aldrich) to reduce any disulfide bonds present. We diluted this mixture to 500 nM in PBS. Immediately after roughening, we submerged the cleaned electrodes in the aptamer solution for 1 h for probe immobilization under dark conditions at room temperature. We follow with an additional passivation step, immersing the gold electrode in 35 mM 6-mercapto-1-hexanol suspended in PBS for 10 to 12 h.

Prior to storing our working electrodes, we ensured they were working properly by collecting 50 scans of square-wave data at 100 Hz using the parameters described above to confirm that the methylene blue peak for each sensor was (i) observable and (ii) not drifting significantly over time. Of the 140 sensors fabricated for storage, none were removed from the study for these reasons.

We next determined the aptamer packing density by collecting cyclic voltammograms between −0.1 V and −0.45 V at a scan a scan rate of 0.1 V s^{-1}, which results in the reduction of all surface-bound methylene blue reporters. We then obtained the total charge associated with reporter-modified aptamers by integrating the area under the reductive curve and dividing this value by the scan rate. We converted this charge to moles of reporter present; dividing this value by the electroactive surface area, as described above, further yielded the packing density.

Electrochemical interrogation

We performed all electrochemical interrogation of our electrodes on a CH Instrument Multipotentiostat CHI1040C (Austin, TX). All measurements utilized a three-electrode setup in which fabricated gold sensors served as the working electrode, a silver/silver chloride aqueous electrode in saturated KCl (CH Instruments) served as the reference electrode, and a platinum wire (CH Instruments) completed the cell as the counter electrode. We used square wave voltammetry to interrogate our electrochemical cell. To do so, we applied a square-wave potential of 25 mV amplitude over the potential window −0.1 V to −0.45 V *versus* a silver/silver chloride reference electrode. We collected data at several square-wave frequencies over the range 3 Hz and 3 kHz. All measurements were conducted at room temperature.

Statistical analysis

We used *t*-tests to compare averaged responses between fresh and stored sensors (at 95% confidence) with no assumption of equal variances between sample populations.

Conflicts of interest

The authors declare the following competing financial interest(s): One author (KWP) has a financial interest in and serves on the scientific advisory board of a company attempting to commercialize EAB sensors. Following the completion of this work, two authors (KKL and JG) became employees of a company attempting to commercialize EAB sensors.

Acknowledgements

This work was funded by NIH grant R01AI145206, by the Otis Williams Postdoctoral Fellowship Fund (CF), and the Department of Defense through the National Defense Science and Engineering Graduate Fellowship (NE).

References

1 A. E. G. Cass, G. Davis, G. D. Francis, H. A. O. Hill, W. J. Aston, I. J. Higgins, E. V. Plotkin, L. D. L. Scott and A. P. F. Turner, Ferrocene-Mediated Enzyme Electrode for Amperometric Determination of Glucose, *Anal. Chem.*, 1984, **56**(4), 667–671, DOI: **10.1021/ac00268a018**.

2 J. Wang, Glucose Biosensors: 40 Years of Advances and Challenges, *Electroanalysis*, 2001, **13**(12), 983–988, DOI: **10.1002/1521-4109(200108)13:12<983::AID-ELAN983>3.0.CO;2-#**.

3 A. Heller and B. Feldman, Electrochemical Glucose Sensors and Their Applications in Diabetes Management, *Chem. Rev.*, 2008, **108**(7), 2482–2505, DOI: **10.1021/cr068069y**.

4 E.-H. Yoo and S.-Y. Lee, Glucose Biosensors: An Overview of Use in Clinical Practice, *Sensors*, 2010, **10**(5), 4558–4576, DOI: **10.3390/s100504558**.

5 P. E. Laibinis, G. M. Whitesides, D. L. Allara, Y. T. Tao, A. N. Parikh and R. G. Nuzzo, Comparison of the Structures and Wetting Properties of Self-Assembled Monolayers of n-Alkanethiols on the Coinage Metal Surfaces, Copper, Silver, and Gold, *J. Am. Chem. Soc.*, 1991, **113**(19), 7152–7167, DOI: **10.1021/ja00019a011**.

6 U. Akiba and M. Fujihira, Preparation of Self-Assembled Monolayers(SAMs) on Au and Ag, in *Encyclopedia of Electrochemistry*, American Cancer Society, 2007, DOI: 10.1002/9783527610426.bard100121.
7 T. Böcking, K. A. Kilian, K. Gaus and J. J. Gooding, Single-Step DNA Immobilization on Antifouling Self-Assembled Monolayers Covalently Bound to Silicon(111), *Langmuir*, 2006, **22**(8), 3494–3496, DOI: 10.1021/la060331a.
8 Y. Xiao, R. Y. Lai and K. W. Plaxco, Preparation of Electrode-Immobilized, Redox-Modified Oligonucleotides for Electrochemical DNA and Aptamer-Based Sensing, *Nat. Protoc.*, 2007, **2**(11), 2875–2880, DOI: 10.1038/nprot.2007.413.
9 P. Dauphin-Ducharme, N. Arroyo-Currás, R. Adhikari, J. Somerson, G. Ortega, D. E. Makarov and K. W. Plaxco, Chain Dynamics Limit Electron Transfer from Electrode-Bound, Single-Stranded Oligonucleotides, *J. Phys. Chem. C*, 2018, **122**(37), 21441–21448, DOI: 10.1021/acs.jpcc.8b06111.
10 N. Arroyo-Currás, J. Somerson, P. A. Vieira, K. L. Ploense, T. E. Kippin and K. W. Plaxco, Real-Time Measurement of Small Molecules Directly in Awake, Ambulatory Animals, *Proc. Natl. Acad. Sci. U. S. A.*, 2017, **114**(4), 645–650, DOI: 10.1073/pnas.1613458114.
11 D. Zhang, J. Ma, X. Meng, Z. Xu, J. Zhang, Y. Fang and Y. Guo, Electrochemical Aptamer-Based Microsensor for Real-Time Monitoring of Adenosine in Vivo, *Anal. Chim. Acta*, 2019, **1076**, 55–63, DOI: 10.1016/j.aca.2019.05.035.
12 K. L. Ploense, P. Dauphin-Ducharme, N. Arroyo-Curras, S. Williams, N. Schwarz, T. Kippin and K. W. Plaxco, Real-Time Pharmacokinetic and Pharmacodynamic Measurements of Drugs within the Brains of Freely Behaving Rats, *FASEB J.*, 2020, **34**(S1), 1, DOI: 10.1096/fasebj.2020.34.s1.07174.
13 F. Tehrani, H. Teymourian, B. Wuerstle, J. Kavner, R. Patel, A. Furmidge, R. Aghavali, H. Hosseini-Toudeshki, C. Brown, F. Zhang, K. Mahato, Z. Li, A. Barfidokht, L. Yin, P. Warren, N. Huang, Z. Patel, P. P. Mercier and J. Wang, An Integrated Wearable Microneedle Array for the Continuous Monitoring of Multiple Biomarkers in Interstitial Fluid, *Nat. Biomed. Eng.*, 2022, **6**(11), 1214–1224, DOI: 10.1038/s41551-022-00887-1.
14 Y. Wu, F. Tehrani, H. Teymourian, J. Mack, A. Shaver, M. Reynoso, J. Kavner, N. Huang, A. Furmidge, A. Duvvuri, Y. Nie, L. M. Laffel, F. J. I. Doyle, M.-E. Patti, E. Dassau, J. Wang and N. Arroyo-Currás, Microneedle Aptamer-Based Sensors for Continuous, Real-Time Therapeutic Drug Monitoring, *Anal. Chem.*, 2022, **94**(23), 8335–8345, DOI: 10.1021/acs.analchem.2c00829.
15 J.-C. Chien, S. W. Baker, K. Gates, J.-W. Seo, A. Arbabian and H. T. Soh, *Wireless Monitoring of Small Molecules on a Freely-Moving Animal Using Electrochemical Aptamer Biosensors*, IEEE, Taipei, Taiwan, 2022, pp. 36–39, DOI: 10.1109/BioCAS54905.2022.9948586.
16 S. Lin, X. Cheng, J. Zhu, B. Wang, D. Jelinek, Y. Zhao, T.-Y. Wu, A. Horrillo, J. Tan, J. Yeung, W. Yan, S. Forman, H. A. Coller, C. Milla and S. Emaminejad, Wearable Microneedle-Based Electrochemical Aptamer Biosensing for Precision Dosing of Drugs with Narrow Therapeutic Windows, *Sci. Adv.*, 2022, **8**(38), eabq4539, DOI: 10.1126/sciadv.abq4539.
17 D. Kang, F. Ricci, R. J. White and K. W. Plaxco, Survey of Redox-Active Moieties for Application in Multiplexed Electrochemical Biosensors, *Anal. Chem.*, 2016, **88**(21), 10452–10458, DOI: 10.1021/acs.analchem.6b02376.
18 T. N. Huan, T. Ganesh, K. S. Kim, S. Kim, S.-H. Han and H. Chung, A Three-Dimensional Gold Nanodendrite Network Porous Structure and Its Application for an Electrochemical Sensing, *Biosens. Bioelectron.*, 2011, **27**(1), 183–186, DOI: 10.1016/j.bios.2011.06.011.
19 S. Wang, Y. Wu, Y. Gu, T. Li, H. Luo, L.-H. Li, Y. Bai, L. Li, L. Liu, Y. Cao, H. Ding and T. Zhang, Wearable Sweatband Sensor Platform Based on Gold Nanodendrite Array as Efficient Solid Contact of Ion-Selective Electrode, *Anal. Chem.*, 2017, **89**(19), 10224–10231, DOI: 10.1021/acs.analchem.7b01560.
20 K. K. Leung, J. Gerson, N. Emmons, J. M. Heemstra, T. E. Kippin and K. Plaxco, The Use of Xenonucleic Acids Significantly Reduces the In Vivo Drift of Electrochemical Aptamer-Based Sensors, *Angew. Chem., Int. Ed.*, 2024, e202316678, DOI: 10.1002/anie.202316678.
21 C. A. Widrig, C. Chung and M. D. Porter, The Electrochemical Desorption of N-Alkanethiol Monolayers from Polycrystalline Au and Ag Electrodes, *J. Electroanal. Chem. Interfacial Electrochem.*, 1991, **310**(1), 335–359, DOI: 10.1016/0022-0728(91)85271-P.
22 K. K. Leung, A. M. Downs, G. Ortega, M. Kurnik and K. W. Plaxco, Elucidating the Mechanisms Underlying the Signal Drift of Electrochemical Aptamer-Based Sensors in Whole Blood, *ACS Sens.*, 2021, **6**(9), 3340–3347, DOI: 10.1021/acssensors.1c01183.
23 R. Y. Lai, D. S. Seferos, A. J. Heeger, G. C. Bazan and K. W. Plaxco, Comparison of the Signaling and Stability of Electrochemical DNA Sensors Fabricated from 6- or 11-Carbon Self-Assembled Monolayers †, *Langmuir*, 2006, **22**(25), 10796–10800, DOI: 10.1021/la0611817.
24 R. J. White and K. W. Plaxco, Exploiting Binding-Induced Changes in Probe Flexibility for the Optimization of Electrochemical Biosensors, *Anal. Chem.*, 2010, **82**(1), 73–76, DOI: 10.1021/ac902595f.
25 B. S. Ferguson, D. A. Hoggarth, D. Maliniak, K. Ploense, R. J. White, N. Woodward, K. Hsieh, A. J. Bonham, M. Eisenstein, T. Kippin, K. W. Plaxco and H. T. Soh, Real-Time, Aptamer-Based Tracking of Circulating Therapeutic Agents in Living Animals, *Sci. Transl. Med.*, 2013, **5**(213), 213ra165, DOI: 10.1126/scitranslmed.3007095.
26 N. V. Ivanova and M. L. Kuzmina, Protocols for Dry DNA Storage and Shipment at Room Temperature, *Mol. Ecol. Resour.*, 2013, **13**(5), 890–898, DOI: 10.1111/1755-0998.12134.
27 N. Phares, R. J. White and K. W. Plaxco, Improving the Stability and Sensing of Electrochemical Biosensors by Employing Trithiol-Anchoring Groups in a Six-Carbon Self-Assembled Monolayer, *Anal. Chem.*, 2009, **81**(3), 1095–1100, DOI: 10.1021/ac8021983.
28 Z. Li, R. Jin, C. A. Mirkin and R. L. Letsinger, Multiple Thiol-Anchor Capped DNA–Gold Nanoparticle Conjugates, *Nucleic Acids Res.*, 2002, **30**(7), 1558–1562.

29 M. Friedel, B. Werbovetz, A. Drexelius, K. Plaxco and J. Heikenfeld, Continuous Molecular Monitoring of Human Dermal Interstitial Fluid with Microneedle-Enabled Electrochemical Aptamer Sensors, *ChemRxiv*, 2023, preprint, DOI: **10.26434/chemrxiv-2023-kplr0**.

30 M. Friedel, B. Werbovetz, A. Drexelius, Z. Watkins, A. Bali, K. W. Plaxco and J. Heikenfeld, Continuous Molecular Monitoring of Human Dermal Interstitial Fluid with Microneedle-Enabled Electrochemical Aptamer Sensors, *Lab Chip*, 2023, **23**(14), 3289–3299, DOI: **10.1039/D3LC00210A**.

31 P. Dauphin-Ducharme, K. Yang, N. Arroyo-Currás, K. L. Ploense, Y. Zhang, J. Gerson, M. Kurnik, T. E. Kippin, M. N. Stojanovic and K. W. Plaxco, Electrochemical Aptamer-Based Sensors for Improved Therapeutic Drug Monitoring and High-Precision, Feedback-Controlled Drug Delivery, *ACS Sens.*, 2019, **4**(10), 2832–2837, DOI: **10.1021/acssensors.9b01616**.

32 C. D. Bain and G. M. Whitesides, Molecular-Level Control over Surface Order in Self-Assembled Monolayer Films of Thiols on Gold, *Science*, 1988, **240**(4848), 62–63, DOI: **10.1126/science.240.4848.62**.

33 C. D. Bain, E. B. Troughton, Y. T. Tao, J. Evall, G. M. Whitesides and R. G. Nuzzo, Formation of Monolayer Films by the Spontaneous Assembly of Organic Thiols from Solution onto Gold, *J. Am. Chem. Soc.*, 1989, **111**(1), 321–335, DOI: **10.1021/ja00183a049**.

34 J. B. Schlenoff, M. Li and H. Ly, Stability and Self-Exchange in Alkanethiol Monolayers, *J. Am. Chem. Soc.*, 1995, **117**(50), 12528–12536, DOI: **10.1021/ja00155a016**.

35 G. G. Baralia, A.-S. Duwez, B. Nysten and A. M. Jonas, Kinetics of Exchange of Alkanethiol Monolayers Self-Assembled on Polycrystalline Gold, *Langmuir*, 2005, **21**(15), 6825–6829, DOI: **10.1021/la050245v**.

36 M. H. Schoenfisch and J. E. Pemberton, Air Stability of Alkanethiol Self-Assembled Monolayers on Silver and Gold Surfaces, *J. Am. Chem. Soc.*, 1998, **120**(18), 4502–4513, DOI: **10.1021/ja974301t**.

37 T. M. Willey, A. L. Vance, T. van Buuren, C. Bostedt, L. J. Terminello and C. S. Fadley, Rapid Degradation of Alkanethiol-Based Self-Assembled Monolayers on Gold in Ambient Laboratory Conditions, *Surf. Sci.*, 2005, **576**(1–3), 188–196, DOI: **10.1016/j.susc.2004.12.022**.

38 T. Laiho and J. A. Leiro, Influence of Initial Oxygen on the Formation of Thiol Layers, *Appl. Surf. Sci.*, 2006, **252**(18), 6304–6312, DOI: **10.1016/j.apsusc.2005.08.037**.

39 A. Brady-Boyd, R. O'Connor, S. Armini, V. Selvaraju, M. Pasquali, G. Hughes and J. Bogan, The Role of Atomic Oxygen in the Decomposition of Self-Assembled Monolayers during Area-Selective Atomic Layer Deposition, *Appl. Surf. Sci.*, 2022, **586**, 152679, DOI: **10.1016/j.apsusc.2022.152679**.

40 K.-A. Yang, R. Pei and M. N. Stojanovic, In Vitro Selection and Amplification Protocols for Isolation of Aptameric Sensors for Small Molecules, *Methods*, 2016, **106**, 58–65, DOI: **10.1016/j.ymeth.2016.04.032**.

41 A. M. Downs, J. Gerson, K. L. Ploense, K. W. Plaxco and P. Dauphin-Ducharme, Subsecond-Resolved Molecular Measurements Using Electrochemical Phase Interrogation of Aptamer-Based Sensors, *Anal. Chem.*, 2020, **92**(20), 14063–14068, DOI: **10.1021/acs.analchem.0c03109**.